

## Title Page

Miting Du (1)

(1) Radioisotope Science and Technology Division, Oak Ridge National Laboratory, Oak Ridge, TN 37831

[mdu1@ornl.gov](mailto:mdu1@ornl.gov)

NOTICE THIS IS A PART OF A SPECIAL ISSUE

MARC XII Assigned Log Number: **204**

*This manuscript has been authored by UT-Battelle LLC under contract DE-AC05-00OR22725 with the US Department of Energy (DOE). The US government retains and the publisher, by accepting the article for publication, acknowledges that the US government retains a nonexclusive, paid-up, irrevocable, worldwide license to publish or reproduce the published form of this manuscript, or allow others to do so, for US government purposes. DOE will provide public access to these results of federally sponsored research in accordance with the DOE Public Access Plan (<http://energy.gov/downloads/doe-public-access-plan>).*

## Applications of a Dual-Column Technique in Actinide Separations

Miting Du

Radioisotope Science and Technology Division, Oak Ridge National Laboratory, Oak Ridge, TN 37831, USA

### ABSTRACT

Selective separation of an individual actinide of interest from other actinides and accompanying lanthanides is a challenging task in radiochemistry and radioanalytical chemistry. This paper illustrates a dual-column technique (i.e., stacked columns of two appropriate resins) to separate an individual actinide of interest, where the selection of two resins and a common effluent running through the stacked columns are key parameters in design of an appropriate dual column. This paper describes the dual column design and practice with two examples, one for a heavy actinide  $^{249}\text{Bk}$  and the other for a light actinide  $^{230}\text{U}$ . In the former case, stacked columns of anion exchange (AX) resin and LN resin replaced the tradition CX-AHIB method used at Oak Ridge National Laboratory for 60 years. In the latter case, an elution process with an AX column followed with a stacked column of AX resin and a DGA resin was applied, instead of traditional methods, e.g., PUREX or U-TEVA methods. Application results of the dual column method to the two example actinides are displayed, while the considerations in method design and the required conditions are discussed.

Key Words: *f*-element separation, CX-AHIB method, dual-column method,  $\text{NaBrO}_4$

## Introduction

Separations of *f*-elements (i.e., lanthanides and actinides) are major tasks in the radioisotope industry. Because of only minute differences between lanthanides and between actinides (i.e., their electronic structure changes are within the *4f* or *5f* inner electron shell instead of the *s* and *p* shells), their mutual separations are always challenging topics in nuclear chemistry studies (Fig. 1).

Lanthanoids	138.905 57 La Lanthanum	140.115 58 Ce Cerium	148.908 59 Pr Praseodymium	144.24 60 Nd Neodymium	144.913 61 Pm Promethium	150.36 62 Sm Samarium	151.960 63 Eu Europium	152.25 64 Gd Gadolinium	158.905 65 Tb Terbium	162.50 66 Dy Dysprosium	164.93 67 Ho Holmium	167.26 68 Er Erbium	168.934 69 Tm Thulium	173.05 70 Yb Ytterbium	174.97 71 Lu Lutetium
	4f <sup>0</sup> 5d <sup>1</sup> 6s <sup>2</sup>	4f <sup>2</sup> 5d <sup>0</sup> 6s <sup>2</sup>	4f <sup>3</sup> 5d <sup>0</sup> 6s <sup>2</sup>	4f <sup>4</sup> 5d <sup>0</sup> 6s <sup>2</sup>	4f <sup>5</sup> 5d <sup>0</sup> 6s <sup>2</sup>	4f <sup>6</sup> 5s <sup>2</sup>	4f <sup>7</sup> 6s <sup>2</sup>	4f <sup>7</sup> 5d <sup>1</sup> 6s <sup>2</sup>	4f <sup>9</sup> 6s <sup>2</sup>	4f <sup>10</sup> 6s <sup>2</sup>	4f <sup>11</sup> 6s <sup>2</sup>	4f <sup>12</sup> 6s <sup>2</sup>	4f <sup>13</sup> 6s <sup>2</sup>	4f <sup>14</sup> 6s <sup>2</sup>	4f <sup>14</sup> 5d 16s <sup>2</sup>
Actinoids	227.028 89 Ac Actinium	231.036 90 Th Thorium	231.028 91 Pa Protactinium	231.028 92 U Uranium	237.048 93 Np Neptunium	244.054 94 Pu Plutonium	243.051 95 Am Americium	247.077 96 Cm Curium	247.077 97 Bk Berkelium	251.068 98 Cf Californium	257.083 99 Es Einsteinium	257.095 100 Fm Fermium	258.1 101 Md Mendelevium	258.1 102 No Nobelium	262.11 103 Lr Lawrencium
	5f <sup>0</sup> 6d <sup>1</sup> 7s <sup>2</sup>	6d <sup>2</sup> 7s <sup>2</sup>	5f <sup>1</sup> 6d <sup>0</sup> 7s <sup>2</sup>	5f <sup>2</sup> 6d <sup>0</sup> 7s <sup>2</sup>	5f <sup>3</sup> 6d <sup>0</sup> 7s <sup>2</sup>	5f <sup>4</sup> 7s <sup>2</sup>	5f <sup>7</sup> 7s <sup>2</sup>	5f <sup>7</sup> 6d <sup>1</sup> 7s <sup>2</sup>	5f <sup>9</sup> 7s <sup>2</sup>	5f <sup>10</sup> 7s <sup>2</sup>	5f <sup>11</sup> 7s <sup>2</sup>	5f <sup>12</sup> 7s <sup>2</sup>	5f <sup>13</sup> 7s <sup>2</sup>	5f <sup>14</sup> 7s <sup>2</sup>	5f <sup>14</sup> 6d 17s <sup>2</sup>

Fig. 1. *f*-elements and the difference in their electronic structures.

In 1956 Gregory. R. Choppin established the cation exchange of  $\alpha$ -hydroxyisobutyric acid (CX-AHIB) process [1] for separation of lanthanides, where a CX column was employed with a mobile fluent containing a water-soluble carboxylate acid complexing reagent, typically AHIB. The strength of the AHIB complexation with each *f*-element increases with the charge density of these trivalent actinide (An) ions or lanthanide (Ln) ions (i.e., the size of these trivalent ions). The resulting affinity of these AHIB-complexed trivalent ions to CX resin deceases in the same order. Due to competing forces from the fixed resin binding sites of  $\text{SO}_3^-$  and from the mobile carboxylate anions  $\text{R}_1\text{R}_2\text{C}(\text{OH})\text{CO}_2^-$ , lanthanide or actinide are eluted off the CX resin column in an order from heavier to lighter in a chromatographic elution process (Fig. 2). The complexing strength of water-soluble carboxylates are pH dependent. In the past 60 years, more carboxylates and other water-soluble complexing agents have been tested and included in this category, so all these are addressed as CX-AHIB type processes.

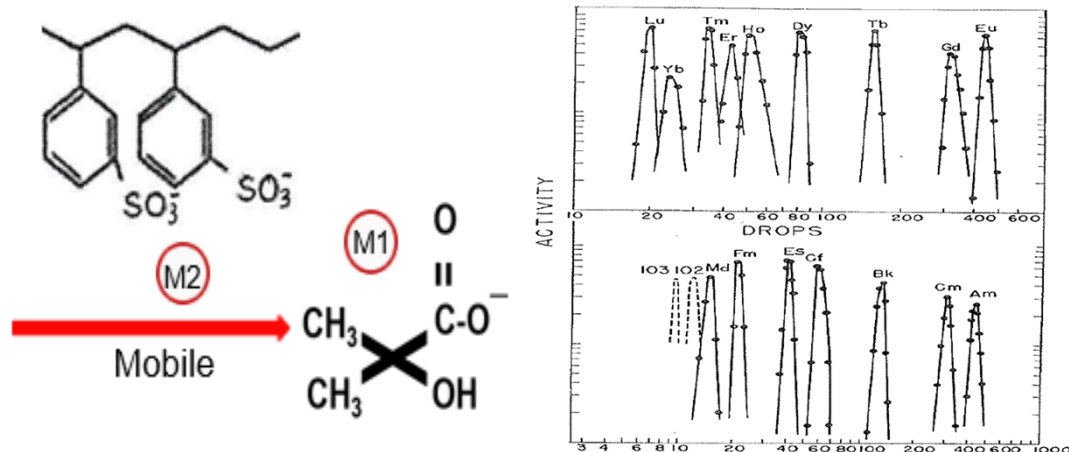


Fig. 2. *f*-elements are chromatographically separated by CX-AHIB type methods [1].

The CX-AHIB method works well, and it has been continuously used over the past 60 years, especially when multiple actinides or lanthanides need to be chromatographically separated on one separatory column (e.g., the initial separations of heavy actinides of Fm, Es, Bk and Cm in Oak Ridge National Laboratory's (ORNL's) Cf-252 Campaigns). Meanwhile some disadvantages of the CX-AHIB method used in routine separation/purification of individual actinide result from its lengthy operations.

The CX-AHIB process comprises at least three column run steps in one cycle: (1) the concentration column run to provide the follow-up chromatographic run with a feed solution of concentrated lanthanides or actinides in a small volume; (2) the chromatographic run with a column of sufficient length; and (3) an additional run to remove AHIB or other complexing agents from the fraction of the separated actinides or lanthanides of interest. The irradiation- or fission-produced actinides are always accompanied by fission product (FP) lanthanides as impurities; therefore, the separated specific actinide fraction by CX-AHIB run always contains a few FP lanthanides, which requires additional column runs for removal of these FP lanthanides from the specific actinides.

The quality of actinide separation by CX-AHIB requires a long column for a chromatographic run with careful controls on the pH of the effluents (for variation of the complexing power of the AHIB) to cater to actinides off the column with desired peak distances (i.e., high separation factors) in an order from heavier to lighter trivalent actinide ions (or from smaller to larger ions). Even with an alpha probe in a hot cell or glove box, the accurate fraction cut to achieve a desired clean actinide is more art than science. Most often, a second set (another three runs) of column runs, even a third set, may become necessary, especially in cases of an insufficiently long column or lack of an alpha probe for online peak detection in the chromatographic run and fraction cuts.

When the goal actinides are more than three for being separated or purified on a same column in a chromatographic manner, the CX-AHIB method is a perfect choice. However, when the goal actinides are fewer than three, lengthy operations of the CX-AHIB method would make radiochemists prefer using separation methods other than CX-AHIB.

In the past 60 years, many new extractants or resins have been invented, giving rise to new methods for selectively separating actinides. This manuscript introduces a new method, named the dual-column technique for separating specific actinides from others and accompanying FP lanthanides in an efficient manner. Two examples of the dual-column application are presented, one for  $^{249}\text{Bk}$  separation from other actinides and impurities as part of the Cf-252 Campaign being undertaken at Oak Ridge National Laboratory, the other for  $^{230}\text{U}$  separation from  $^{232}\text{Th}$ ,  $^{230}\text{Pa}$ , and other impurities, towards a new generator  $^{230}\text{U}/^{226}\text{Th}$  study.

The general concept of a dual-column method for actinide separation is simple in its design: stack two columns of different resins in a vertical configuration and run the feed of impure actinides through the stacked columns with follow-up elution. The key point of a stacked-column design to separate a specific actinide from others is to choose two complementary resins and common mobile effluent running through the stacked columns to selectively absorb the target

actinide and strip it off free of contaminants. The columns in use must be detachable, with features satisfying requirements; for example, the columns may need a water jacket to maintain the required temperatures or a design that allows for driving effluent through a syringe or by air pressure (Fig. 3).



**Fig. 3.** Examples of attachable columns for requirements of volume, temperature and effluent loading.

Two examples of such dual-column applications for a specific actinide separation undertaken in recent years at ORNL are described below: one for  $^{249}\text{Bk}$  (a heavy actinide) and the other for  $^{230}\text{U}$  (a light actinide), separated from other actinides and impurities.

## Experimental Methods

### Reagents, Resins, Column Preparations

Nitric acid (69–70% ACS Grade,  $\text{HNO}_3$ ) was purchased from BDH. Hydrochloric acid (37%, Trace Metals grade) was purchased from RICCA Chemical Company. Hydrogen peroxide (30%,  $\text{H}_2\text{O}_2$ ) was purchased from Fisher Chemical. Hydrofluoric acid (40%) was purchased from EMD Millipore Corp. 2M  $\text{NaBrO}_3$  was prepared with solid  $\text{NaBrO}_3$  of >99% purity purchased from ACROS Organics. The Bio-Rad® MP-1 resin with a particle size of 100–200 mesh was purchased from Bio-Rad Laboratories. Eichrom® LN resin and DGA resin (normal) with a particle size of 100–150  $\mu\text{m}$  were purchased from Eichrom Tech Inc. The 2 mL plastic cartridge used for column assembly were purchased from Eichrom Tech Inc. The Eichrom LN and DGA columns were prepared by directly loading dry resins into the 2 mL cartridge and then wetting with 2 M  $\text{HNO}_3$  and deionized (DI) water and, finally, conditioning with selected effluent prior to use. The MP-1 columns were prepared by loading DI water-wetted resin into 2 mL cartridges and then conditioning with selected effluent prior to use.

### Sample Analyses

The Transuranium Analytical Laboratory (TAL) at ORNL's Radiochemical Engineering Development Center (REDC) is equipped with radiological analysis equipment including high-purity germanium (HPGe) gamma spectrometers; alpha spectrometers (i.e., Passivated Implanted Planar Silicon detectors); and inductively couple plasma mass spectrometry (ICP-MS) (Thermo Fisher iCAP Q). Samples for  $^{249}\text{Bk}$  were measured by a gas-flow proportional counter based on calibrations with a  $^{249}\text{Bk}$  sample premeasured with a Perkin Elmer 5110TR liquid scintillation counter in another laboratory.

Samples of  $^{249}\text{Cf}$  were measured by both gross alpha and gamma spectrometric methods, based on the alpha energies of 5.78 MeV (0.26%) and 5.81 MeV (82.2%) and the gamma energies of 333.5 keV and 388.3 keV.

Samples for  $^{141,144}\text{Ce}$  were measured by gamma spectrometric method, based on their typical gamma energies of 145.4 keV ( $^{141}\text{Ce}$ ) and 133.5 keV ( $^{144}\text{Ce}$ ). Part of the samples of  $^{249}\text{Cf}$  and  $^{141,144}\text{Ce}$  were measured with a GMX-25 Coaxial HPGe gamma spectrometer, based on their typical gamma energies at a relatively high background laboratory environment.

Samples of  $^{230}\text{U}$  were measured by both gross alpha and gamma spectrometric methods, based on the alpha energies of 5.818 MeV (32.0%) and 5.889 MeV (67.4%) and the daughters' gamma energies of 111.1 keV ( $^{226}\text{Th}$ , 3.29%), 324.5 keV ( $^{222}\text{Ra}$ , 2.77%), and 609.3 keV ( $^{218}\text{Rn}$ , 0.124%).

Samples of  $^{230}\text{Pa}$  were measured by gamma spectrometric methods, based on the gamma energies of \*951.88 keV (30 $\pm$ 3%), 918.5 keV (8.3 $\pm$ 0.7%), 454.9 keV (6.8 $\pm$ 0.6%), 898.6 keV (5.8 $\pm$ 0.5%), and 443.7 keV (5.8 $\pm$ 0.5%). The asterisk denotes a major peak.

## Results and Discussion

### **$^{249}\text{Bk}$**

Producing  $^{249}\text{Bk}$  as a By-product in Cf-252 Campaigns at ORNL

As an important heavy actinide,  $^{249}\text{Bk}$  is produced via successive neutron captures and beta decays of the curium feedstock irradiated in the High Flux Isotope Reactor (HFIR) at ORNL.

**Fig. 4** shows the nuclear reaction route of  $^{249}\text{Bk}$  produced in multiple neutron captures and beta decays in HFIR irradiation, while **Fig. 5** shows the major postirradiation processing steps after target discharge and cooling.

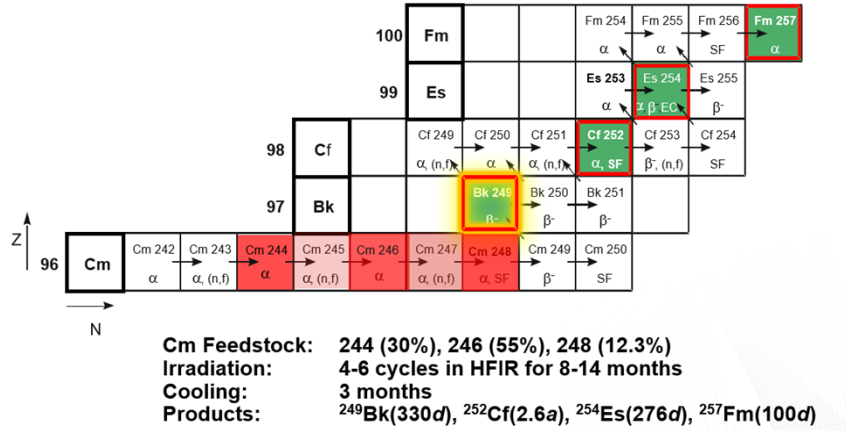


**Fig. 4.**  $^{249}\text{Bk}$  produced by neutron captures and beta decays of irradiated Cm feedstock at HFIR.

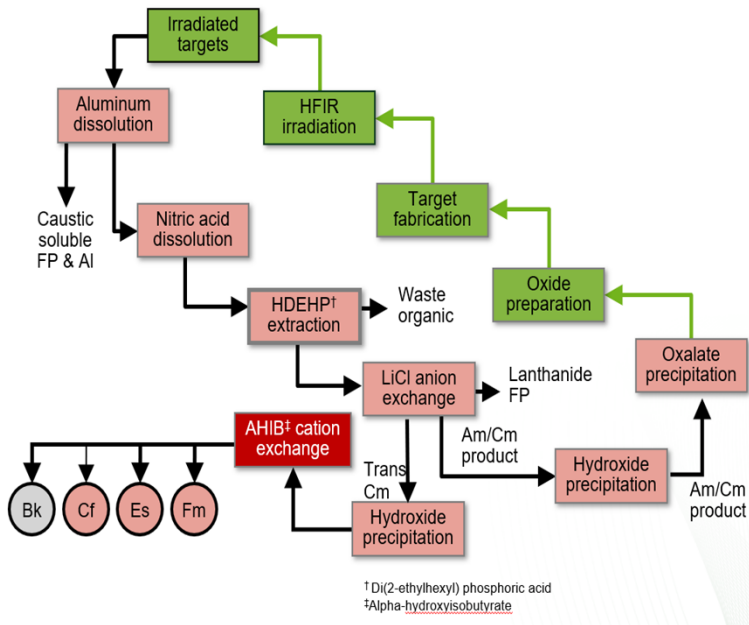


**Fig. 5.** Major steps of the post irradiation processing of the irradiated Cm feedstock target.

The irradiation and post irradiation processes undertaken on the Cm feedstock target at ORNL is addressed in the Cf-252 Campaign [2], with  $^{252}\text{Cf}$  as the major product and  $^{249}\text{Bk}$ ,  $^{254}\text{Es}$ , and  $^{257}\text{Fm}$  as by-products. After completing the steps of caustic dissolution, acidic dissolution, di-(2-ethylhexyl) phosphoric acid (HDEHP) extraction, two times of LiCl anion exchange, and LiOH precipitation, the mixture of  $^{252}\text{Cf}$ ,  $^{249}\text{Bk}$ ,  $^{254}\text{Es}$ ,  $^{257}\text{Fm}$  and residual impurities is processed by the CX-AHIB operations in a hot cell through a concentrator column and a chromatographic column 1.6 m in length. The achieved preliminary separation of these heavy actinides is shown on the elution curve by an alpha flow-through detector in **Fig. 6**.

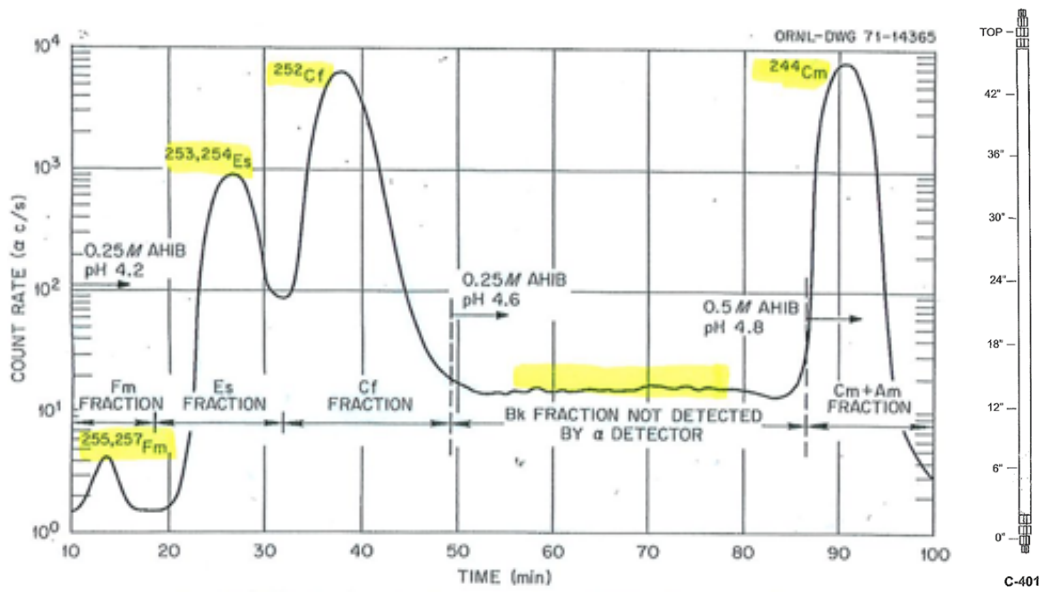


**Fig. 6.** Heavy actinide elution curve drawn by  $\alpha$  flow-through detector [3].

### Original ORNL Process for Bk-249 Finishing

The fraction cuts of this CX-AHIB column run are moved to next steps for further purification of each actinide, addressed as  $^{252}\text{Cf}$  finishing,  $^{249}\text{Bk}$  finishing, and so on. All these purifications rely on using the CX-AHIB method, except for a recent method change of  $^{249}\text{Bk}$  finishing to the dual-column method. The impure fraction of  $^{249}\text{Bk}$  from the hot cell via CX-AHIB contains impurities of Cf, Cm, FP lanthanides, and other metal ion impurities. The original operation steps of  $^{249}\text{Bk}$  finishing after the CX-AHIB in hot cell are described in **Fig. 7**.

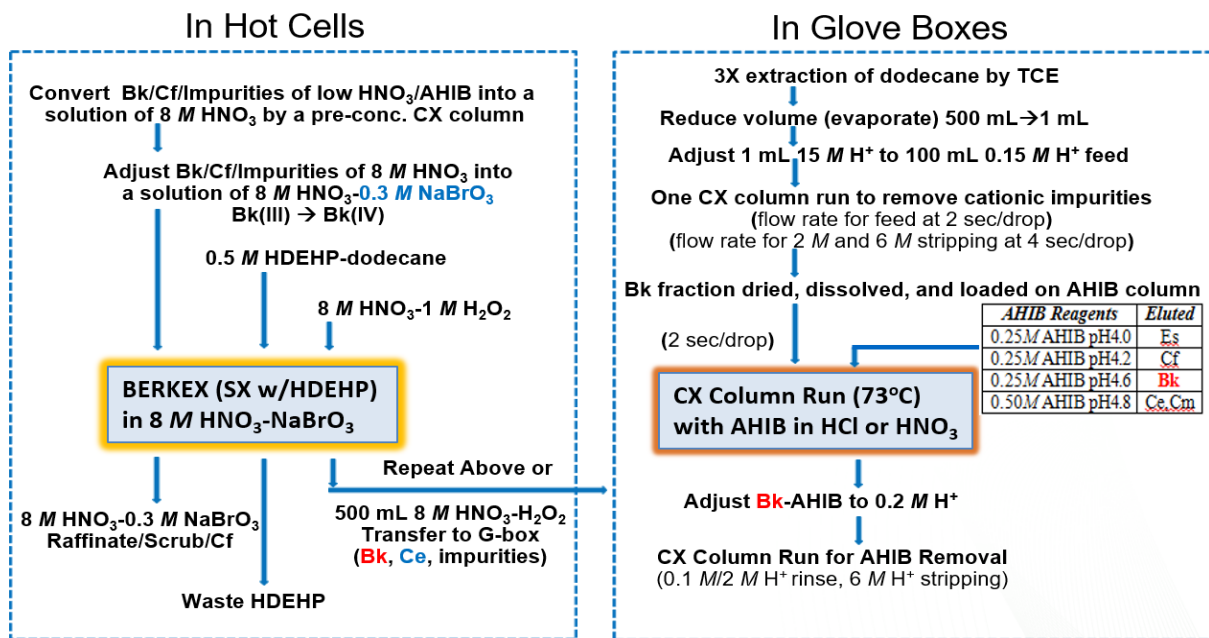


**Fig. 7.** Original  $^{249}\text{Bk}$  finishing steps for BERKEX in hot cell and CX-AHIB in glove box labs.

These operations include BERKEX (operations in hot cell), followed with additional CX-AHIB (operations in glove box). In the BERKEX process, the impure  $^{249}\text{Bk}$  solution is adjusted into 8 M  $\text{HNO}_3$ –0.3 M  $\text{NaBrO}_3$  and mixed with the organic extractant HDEHP, whereas  $\text{Bk}^{3+}$  is oxidized to  $\text{Bk}^{4+}$  by  $\text{BrO}_3^-$  and extracted by HDEHP while other  $\text{An}^{3+}$  remain in their trivalent form and stay in aqueous phase. Among Ln FP, only  $\text{Ce}^{3+}$  will also be oxidized to tetravalent  $\text{Ce}^{4+}$ , extracted with  $\text{Bk}^{4+}$  product, and transferred to glove box labs for further separations by CX-AHIB after being stripped off from HDEHP by 8 M  $\text{HNO}_3$ –0.45 M  $\text{H}_2\text{O}_2$ . BERKEX may have to be run twice prior to transfer to glove box for AHIB operations.

Glove box AHIB operations include residual organic (i.e., dodecane) removal and three (per set) CX column runs: one for preconcentrating all cations to prepare the load for the follow-up AHIB column run; one for separating  $^{249}\text{Bk}$  from others during the CX-AHIB chromatographic column run itself; and one for removing AHIB from the  $^{249}\text{Bk}$  product cut of the glove box AHIB run. The CX-AHIB column run employs AHIB as a competing extractant ( $\text{COO}^-$ ) in the mobile phase to compete with the CX resin ( $\text{SO}_3^-$ )'s power in adsorbing cations. Increasing the strength of AHIB (increasing pH or AHIB concentration) would result in the cations on the column being eluted out in the order of their charge densities. (For actinides of same valence, this would follow the order of their ion sizes (e.g.,  $\text{Fm}^{3+}$ ,  $\text{Es}^{3+}$ ,  $\text{Cf}^{3+}$ , then  $\text{Bk}^{3+}$ ). The operations of CX-AHIB column runs require strict control of pH, flow rate, column temperature, and cutting of the effluent with care. Because the peaks of Bk and Cf are very close in the CX-AHIB column run, a small portion of Cf peak tail may end up being collected into the  $^{249}\text{Bk}$  product cut. **Fig. 8** shows some detailed information on the glove box AHIB run in a previous Cf-252 Campaign.

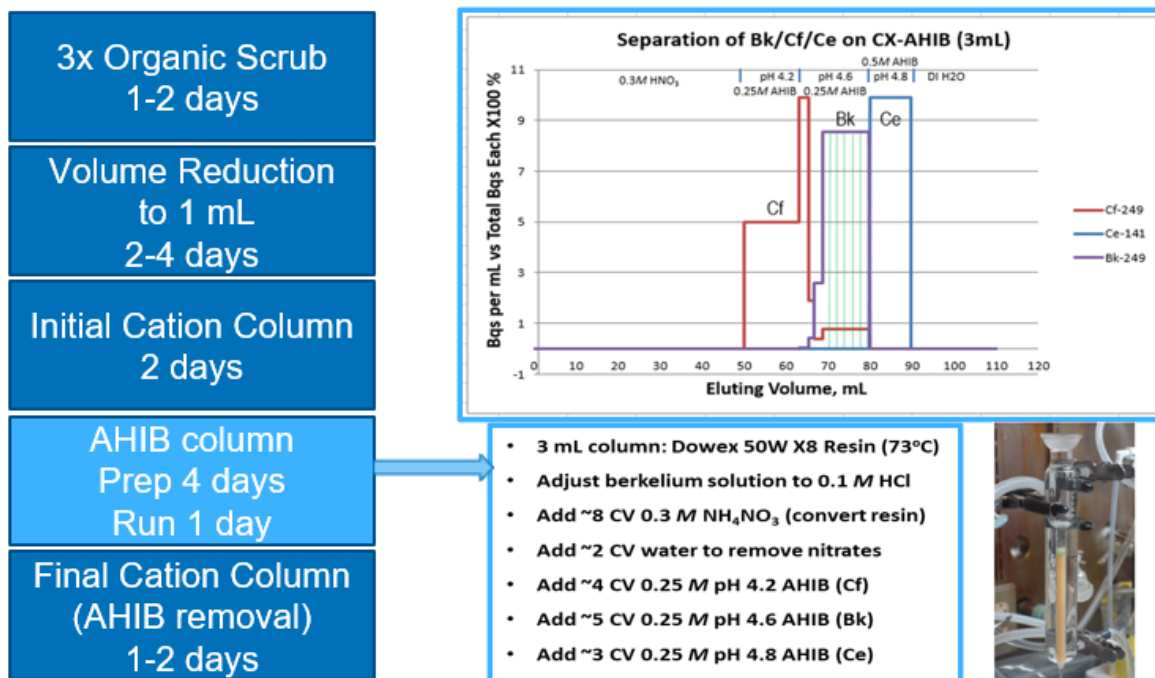


**Fig. 8.** Glove box AHIB column run in a previous campaign and expected operation days.

Expected time for glove box CX-AHIB operations is around 2 weeks, in hopes that the chromatographic column separation of  $^{249}\text{Bk}$  from others can be achieved by one set of column

runs (three runs per set). Comparing the glove box method with the hot cell CX-AHIB process with a chromatographic column of 1.6 m length for a mass throughput of 100 mg, the CX-AHIB process in a glove box allows limited column length (the resin bed is in ~10 cm long) to separate a mass of >20 mg, and no alpha probe is available to aid Cf fraction detection. Moreover, there is no adequate method to detect the  $^{249}\text{Bk}$  on site. Normally, the glove box CX-AHIB process needs a second or even third set of column runs to achieve the required purity of the  $^{249}\text{Bk}$  product.

The AHIB column elution profile in **Fig. 8** shows the run as a chromatographic elution process with strict control of temperature (73°C), pH (4.2, 4.6, and 4.8), and flow rate (counting seconds/drop) with an Ar over pressure. The “fraction cut of  $^{249}\text{Bk}$  product” in this AHIB run (the shaded portion in the top right panel) achieved 94% of  $^{249}\text{Bk}$  recovery from the feed, but also shows 4.1% of Cf carried over from the feed. Due to additional runs, the above  $^{249}\text{Bk}$  finishing took 8 weeks, adding to a total 7 months of processing after the target cooling.

The longer the processing of the irradiated target goes on, the higher the decay loss of the  $^{249}\text{Bk}$  (330 d) product is (e.g., decay loss of 8 weeks to  $^{249}\text{Bk}$  is 11.1%). Therefore, efforts were made to develop new techniques for quicker  $^{249}\text{Bk}$  finishing, leading to the concept of the dual-column method.

### Development of a Dual-Column Method for Bk-249 Finishing

Separation of  $^{249}\text{Bk}$  from Cf, Cm, and FP lanthanides is the key purpose of Bk finishing, while the most common valence state for all these ions in  $\text{HNO}_3$  medium is trivalent. Different from  $\text{Cf}^{3+}$  and  $\text{Cm}^{3+}$ ,  $\text{Bk}^{3+}$  can be oxidized to tetravalent  $\text{Bk}^{4+}$  by  $\text{BrO}_3^-$  and then be extracted by organic extractant HDEHP in  $\geq 7$  M  $\text{HNO}_3$ —if in  $\leq 2$  M  $\text{HNO}_3$ , HDEHP extracts trivalent  $\text{An}^{3+}$ ,  $\text{Ln}^{3+}$  and other  $\text{M}^{3+}$  as well—which has been proved by the BERKEX process. Without light tetravalent actinides (e.g.,  $\text{Th}^{4+}$ ,  $\text{Pu}^{4+}$ ) in the solution,  $^{249}\text{Bk}$  encounters less competition from tetravalent cations and therefore more likely to be efficiently separated from the trivalent  $\text{Cf}^{3+}$ ,  $\text{Cm}^{3+}$ , and  $\text{Ln}^{3+}$  once oxidized from  $\text{Bk}^{3+}$  to  $\text{Bk}^{4+}$  **[4]** (**Table 1**).

**Table 1.** Features of actinide valences in aqueous media.

	89	90	91	92	93	94	95	96	97	98	99	101	102	103	104
+2										$\text{Cf}^{2+}$	$\text{Es}^{2+}$	$\text{Fm}^{2+}$	$\text{Md}^{2+}$	$\text{No}^{3+}$	
+3	$\text{Ac}^{3+}$		$\text{Pa}^{3+}$	$\text{U}^{3+}$	$\text{Np}^{3+}$	$\text{Pu}^{3+}$	$\text{Am}^{3+}$	$\text{Cm}^{3+}$	$\text{Bk}^{3+}$	$\text{Cf}^{3+}$	$\text{Es}^{3+}$	$\text{Fm}^{3+}$	$\text{Md}^{3+}$	$\text{No}^{3+}$	$\text{Ln}^{3+}$
+4		$\text{Th}^{4+}$	$\text{Pa}^{4+}$	$\text{U}^{4+}$	$\text{Np}^{4+}$	$\text{Pu}^{4+}$	$\text{Am}^{4+}$	$\text{Cm}^{4+}$	$\text{Bk}^{4+}$	$\text{Cf}^{4+}$	$\text{Es}^{4+}$				
+5			$\text{PaO}_2^{+}$	$\text{UO}_2^{+}$	$\text{NpO}_2^{+}$	$\text{PuO}_2^{+}$	$\text{AmO}_2^{+}$								
+6				$\text{UO}_2^{2+}$	$\text{NpO}_2^{2+}$	$\text{PuO}_2^{2+}$	$\text{AmO}_2^{2+}$								
+7					$\text{NpO}_2^{3+}$	$\text{PuO}_2^{3+}$									

Green = most common valences; Yellow = reachable valences in aqueous media

Since 2018, several resins have been tested at ORNL with tracers of  $^{249}\text{Bk}$ ,  $^{249}\text{Cf}$ ,  $^{141,144}\text{Ce}$ , and other impurities in the feed of 8 M  $\text{HNO}_3$ –0.5 M  $\text{NaBrO}_3$  solution and followed with same effluent elution [5]. Test results of two resins brought attentions.

**BioRad® MP-1 resin** has been broadly used in radionuclide separations, especially in actinide separations. Cations in aqueous solution are considered hydrated ions (i.e., ions surrounded with  $\text{H}_2\text{O}$  molecules due to the dipolar force of  $\text{H}_2\text{O}$  molecules and the charge density of ions). For cations ( $\text{M}^{n+}$ ) in high concentrations of an acid solution (HA),  $\text{H}_2\text{O}$  molecules of the inner sphere of the cation hydrate ions may be replaced by anions ( $\text{A}^-$ ) of the acid (HA), to further form metal anions (e.g.,  $\text{MA}_m^{(m-n)-}$ ). Actinides, particularly those with higher oxidation states, from Th to Bk, may form actinide anions in high concentrations of  $\text{HCl}$  or  $\text{HNO}_3$  and then may be adsorbed on anion exchange resins. The most familiar examples include Th(IV) in high  $\text{HNO}_3$  (but not in  $\text{HCl}$ ), U(VI) in high  $\text{HCl}$  (but not in  $\text{HNO}_3$ ), and Pu(IV) in either high  $\text{HNO}_3$  or high  $\text{HCl}$ . Bk(IV) has a smaller ionic size than abovementioned tetravalent actinides, indicating higher charge density; therefore, Bk(IV), after being oxidized from Bk(III), can be expected to form anions that are adsorbed onto anion exchange resins.

The test results of the MP-1 column run through with tracers of  $^{249}\text{Bk}$ ,  $^{249}\text{Cf}$ ,  $^{141,144}\text{Ce}$ , and other impurities in the effluent of 8 M  $\text{HNO}_3$ –0.5 M  $\text{NaBrO}_3$  (i.e., an oxidizer) showed only retention of Ce(IV), without Bk(IV), Cf(III), and other impurities. This was an unexpected result. Did the oxidizer  $\text{NaBrO}_3$  fail to oxidize  $\text{Bk}^{3+}$  to  $\text{Bk}^{4+}$  in these tests? Successful BERKEX experience over the past 60 years does not support this opinion. The test with the LN resin column was performed for confirmation.

**Eichrom® LN resins** are porous polymer (Amberchrom® CG71) particles of selected sizes impregnated with HDEHP. The chemistry of the LN resin column run with feed/wash in 8M  $\text{HNO}_3$ – $\text{NaBrO}_3$  is the same in principle as the BERKEX process; the only difference is that the extractant of one is solid resin form while the other is in liquid organic form. A change from a one-stage solvent extraction (SX) to a column run will have the advantage of high plate numbers for  $^{249}\text{Bk}$  adsorption onto LN resins and the lack of the organic liquid (i.e., HDEHP) waste disposal issue, although operation parameters such as  $^{249}\text{Bk}$  amount vs. resin bed size, proper length/diameter of resin bed, and volumes of each fraction cut need to be determined in trial runs.

The column tests with LN resin showed that both  $^{249}\text{Bk}$  and  $^{141,144}\text{Ce}$  were retained on the LN column and later stripped off by lower  $\text{HNO}_3$ –0.45 M  $\text{H}_2\text{O}_2$ . Meanwhile,  $^{249}\text{Cf}^{3+}$  and other impurities of trivalent, divalent, or monovalent ions were eluted off the column during 8M  $\text{HNO}_3$ – $\text{NaBrO}_3$  elution. The retention of both  $^{249}\text{Bk}$  and  $^{141,144}\text{Ce}$  by LN resin in high- $\text{HNO}_3$  media proved that both  $\text{Bk}^{3+}$  and  $\text{Ce}^{3+}$  are oxidized as tetravalent  $\text{Bk}^{4+}$  and  $\text{Ce}^{4+}$  by  $\text{BrO}_3^-$  in the effluent due to their standard reduction potentials ( $E^\circ$ ) being similar.  $E^\circ$  values of  $\text{Ce}^{3+}/\text{Ce}^{4+}$  and  $\text{Bk}^{3+}/\text{Bk}^{4+}$  in **Table 2** prove oxidation and absorption by HDEHP in the BERKEX process.

**Table 2.** Standard reduction potentials ( $E^\circ$ ) of concerned ions.

Half-Reactions	$E^\circ$ (V)
$O_{2(g)} + 2 H^{+}_{(aq)} + 2 e^- \rightleftharpoons H_2O_{2(aq)}$	+0.68
$Br_{2(l)} + 2 e^- \rightleftharpoons 2 Br^{-}_{(aq)}$	+1.07
$Cr_2O_7^{2-}_{(aq)} + 14 H^{+}_{(aq)} + 6 e^- \rightleftharpoons 2 Cr^{3+}_{(aq)} + 7 H_2O$	+1.33
$Cl_{2(l)} + 2 e^- \rightleftharpoons 2 Cl^{-}_{(aq)}$	+1.36
$BrO_3^{-} + 6 H^{+}_{(aq)} + 6 e^- \rightleftharpoons Br^{-}_{(aq)} + 3 H_2O$	+1.44
$Ce^{4+}_{(aq)} + e^- \rightleftharpoons Ce^{3+}_{(aq)}$	+1.61
$Bk^{4+}_{(aq)} + e^- \rightleftharpoons Bk^{3+}_{(aq)}$	+1.67
$H_2O_{2(aq)} + 2 H^{+}_{(aq)} + 2 e^- \rightleftharpoons 2 H_2O$	+1.77

Because both  $Bk^{3+}$  and  $Ce^{3+}$  are oxidized to  $Bk^{4+}$  and  $Ce^{4+}$  in high  $HNO_3$ – $NaBrO_3$  media in BERKEX, the question arose of why  $Ce^{4+}$  is retained on the MP-1 column in the same media while  $Bk^{4+}$  does not? The reasonable answer would be that **in the presence of  $NaBrO_3$ , the tetravalent  $Ce^{4+}$  forms anions in 8 M  $HNO_3$  while  $Bk^{4+}$  does not.**

Further literature studies demonstrated that, early in 1976, ORNL chemist F. L. Moore found this “surprising sorption behavior difference of  $Bk(IV)$  and  $Ce(IV)$  nitrate anions on anion exchange resins” [6] and explained it as “*Bk(IV) forms weaker nitrate anions than Ce(IV) anions because of its smaller ionic radius (0.8 Å) vs. Ce(IV) (0.92 Å).*” He considered the  $Bk(IV)$  nitrate anions were formed but just too weak. In 1979, Russian chemist Makarova et al. [7] ran a comparative electromigration with  $Bk$ ,  $Pu$ ,  $Th$ , and  $Ce$  in a varying  $[HNO_3]$ , from 2 to 16 M, respectively, using  $HNO_3$ – $NaBrO_3$  media in the cases of  $Bk$  and  $Ce$ . They found that “*[7] the mobility corresponding to negatively charged ions in the case of  $Bk(IV)$  appears only at  $HNO_3$  concentrations higher than 10M,*” which works as objective evidence to the current conclusion of “**no  $Bk^{4+}$  anion formation in 8 M  $HNO_3$ – $NaBrO_3$ ,**” suggesting a possibility of anion formation in  $\geq 10$  M  $HNO_3$  in the presence of an oxidizer.

With the knowledge of differences in sorption behavior of the two resins to  $Bk^{4+}$  and other tetravalent actinides/metal ions, a new method of selectively separating  $Bk^{4+}$  from other  $M^{4+}$  and impurities was invented [5]:

*Stack an anion exchange resin (MP-1 was chosen) column on top of a LN resin column and run the feed of crude  $^{249}Bk$  in 8 M  $HNO_3$ –0.5 M  $NaBrO_3$  going through the stacked two columns, where all  $M^{4+}$  (either original existing ones or those being oxidized by  $BrO_3^-$ ), except for  $Bk^{4+}$ , will be retained by the AX column (functioned as a  $M^{4+}$  filter).  $Bk^{4+}$  and all trivalent, divalent and monovalent impurities will pass from the AX column to the LN column, where  $Bk^{4+}$  will be*

*retained by the LN column while impurities of  $M^{<4+}$  going through the LN column (no retention to them due to high  $HNO_3$  media) for disposal.*

This new method was tested with increasing amounts of  $^{249}Bk$  and impurities to determine its operational parameters, such as the  $^{249}Bk$  loading capacity on the LN column, proper length/diameter of the resin bed, and volumes of each fraction cut, prior to its application in the Bk Finishing of the 2021 Cf-252 Campaign.

### Application of the New Technique in the Bk Finishing of Cf-252 Campaign

In the 2021 Cf-252 Campaign, this dual-column technique was used to replace the glove box CX-AHIB operations, while scale up operations for the hot cell processing (BERKEX) are being considered. but not replacing the BERKEX yet because any change of existing hot cell operational procedures takes longer time for an approval.

The 540 mL of 0.5 M  $HNO_3$ – $H_2O_2$  solution containing ~10.7 mg of  $^{249}Bk$  with impurities was transferred from a hot cell to a glove box and scrubbed only once with hexane to remove trace organic HDEHP carried over from the BERKEX process. (By comparison, three scrubbings would be required in the original CX-AHIB operations.) It is important to note that, once the new method replaces the entire Bk finishing (including BERKEX), this organic scrubbing step will not be necessary.

The crude  $^{249}Bk$  solution was dried down for volume reduction from 540 mL+ washes to only a few mL in a setup of flask and heating mantle for evaporation and condensation. Two batches of cool-down condensates were collected: the first batch of large-volume condensate (Cond-1) was low acidity, while the second batch of smaller-volume condensate (Cond-2) was higher acidity. The few mL of impure  $^{249}Bk$  solution, left inside the flask, was considered concentrated  $HNO_3$  due to evaporation and adjusted with prepared 2 M  $NaBrO_3$  solution and DI  $H_2O$  to make a feed of 8 M  $HNO_3$ –0.5 M  $NaBrO_3$ .

Columns were prepared and preconditioned with 8 M  $HNO_3$  prior to the bagging into the glove box. Immediately prior to column operations, the 2 mL MP-1 column was stacked onto the 2 mL LN column and conditioned with 8 M  $HNO_3$ –0.5 M  $NaBrO_3$ . The small volume of prepared feed solution of 8 M  $HNO_3$ –0.5 M  $NaBrO_3$  was then loaded into the top empty syringe in batches and injected into the stacked MP-1/LN column, followed with  $\geq 6$  column volumes (CV) of 8 M  $HNO_3$ –0.5 M  $NaBrO_3$  elution to ensure  $^{249}Bk$  transfer from MP-1 column to LN column and  $M^{<4+}$  impurities going through both columns. This off-column effluent of feed + load + raffinate (FLR) was collected into the bottle marked “FLR” for later analysis of potential  $^{249}Bk$  breakthrough at this step.

The LN column was detached from the top MP-1 column and eluted with  $\geq 4$  mL (2 CV of the LN column) of 8 M  $HNO_3$  to wash  $NaBrO_3$  away from the LN column (away from  $^{249}Bk$ ). This wash was also collected into the bottle marked “FLR”. Until this step,  $^{249}Bk$  should be retained alone on the 2 mL LN column in the medium of 8 M  $HNO_3$  (i.e., without  $M^{<4+}$  impurities and the

oxidizer  $\text{NaBrO}_3$ ). **Fig. 9** illustrates the operation steps, where the green band on the single LN column (see photo panels) shows  $\text{Bk}^{4+}$  position along the column.

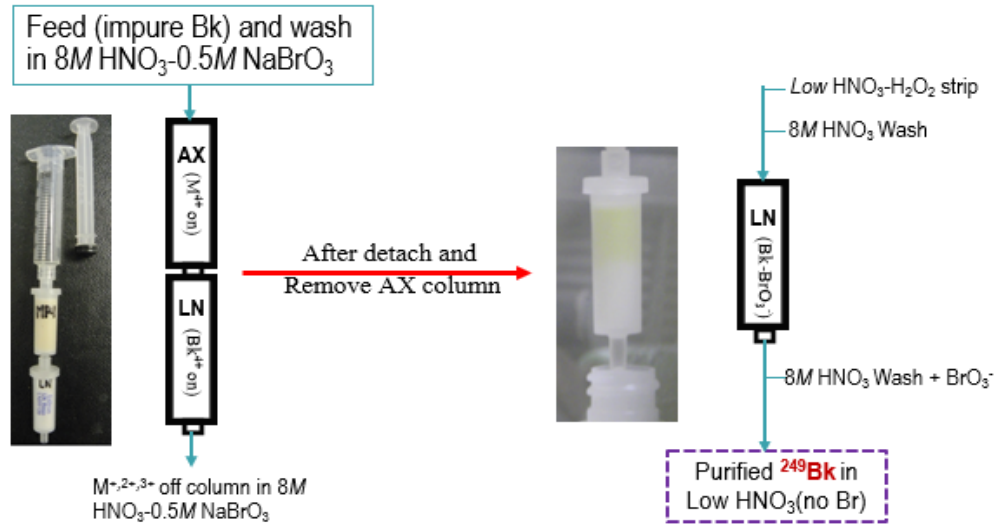


**Fig. 9.** Separating  $^{249}\text{Bk}$  selectively by using a dual-column technique.

The  $^{249}\text{Bk}$  on the LN column was stripped off by 10 CV of low  $\text{HNO}_3$ -0.4 M  $\text{H}_2\text{O}_2$ , while the effluent was collected into the bottle marked “LN Strip”.  $\text{H}_2\text{O}_2$  reduces  $\text{Bk}^{4+}$  to  $\text{Bk}^{3+}$ , while the “low”  $\text{HNO}_3$  should be a compromise of “ease in final drying down” and “quick in Bk stripping” (i.e., affinity of  $\text{Bk}^{3+}$  to LN resin increases with decreased  $\text{HNO}_3$  acidity). 0.3 M  $\text{HNO}_3$ -0.4 M  $\text{H}_2\text{O}_2$  was used for the  $\text{Bk}^{4+}$  stripping in this work.

After the MP-1 column was detached from the LN column, the MP-1 column can be stripped with 5 CV of 0.3 M  $\text{HNO}_3$ -0.4 M  $\text{H}_2\text{O}_2$ , where the  $\text{H}_2\text{O}_2$  reduces  $\text{Ce}^{4+}$  to  $\text{Ce}^{3+}$  (as well  $\text{Bk}^{4+}$ , if present) and low  $\text{HNO}_3$  elutes other impurities off the MP-1 column (e.g.,  $\text{Pu}^{4+}$  if present). In routine campaigns, detached MP-1 columns can be directly disposed of as solid radioactive waste instead of stripping the column to create a radioactive liquid waste.

By end of the Bk finishing process using the new method, five fractions of solutions were collected as Cond-1, Cond-2, FLR, LN strip, and MP-1 strip, from which samples were taken and analyzed. The analytical data are summarized in **Table 3**. After stripping, the two columns had a non-detectable dose above background.

**Table 3.** Calculated isotopes' amounts in fractions based on analytical data.

	Cond-1	Cond-2	subtotal	FLR	LN Strip	MP-1 Strip	subtotal
Vol. (mL)	505	120	625		40	35	4.5
$^{249}\text{Bk}$ (mg)	0.00907	0.223	<b>0.232</b>		0.0164	<b>10.405</b>	0.0464
% subtotal	3.908	96.092	100		0.157	<b>99.4</b>	0.443
$^{141}\text{Ce}$ (Bq)	<DL	2.76E5			1.19E6	<DL	4.32E6
$^{144}\text{Ce}$ (Bq)	<DL	<DL			1.81E6	<DL	1.53E6
G- $\alpha$ (Bq)*	<DL	1.8E6			4.4E7	<DL	6.84E5

\*Gross alpha (5.5, 5.8, 5.95 and 6.11 MeV) indicates  $^{249,251}\text{Cf}$  and some Cm, not beta emitter  $^{249}\text{Bk}$ .

With a total 10.7 mg  $^{249}\text{Bk}$  coming from hot cell BERKEX, 10.405 mg of the final purified  $^{249}\text{Bk}$  in the LN strip shows an overall recovery rate of 97.24%. Not counting the  $^{249}\text{Bk}$  loss (0.232 mg) in the two condensates, the  $^{249}\text{Bk}$  recovery rate during the dual-column run would be as high as 99.4% of the original  $^{249}\text{Bk}$  in the feed solution. Based on the green  $^{249}\text{Bk}$  band (10.4 mg) on a 2 mL column, the Bk loading capacity of a 2 mL LN column should be sufficient for approx. 20 mg of  $^{249}\text{Bk}$  to be retained.

The most significant change in Bk finishing attained using the dual-column method is that processing time—from transfer of the crude  $^{249}\text{Bk}$  solution into the glove box to the product being ready for shipping—was just 8 days, instead of 8 weeks required by the CX-AHIB process.

The US Department of Energy Isotope Program (DOE IP) has approved this dual-column procedure for Bk finishing processing in future Cf-252 Campaigns. This method is also recommended for  $^{249}\text{Bk}$  content analyses of those samples from the beginning steps of the Cf-252 campaigns, (e.g., samples from acid dissolution, HDEHP extraction) (Fig. 3), if the total isotopes in the sample are no more than 1  $\mu\text{g}$  in mass (to avoid the possibility of liquid oxidizer  $\text{BrO}_3^-$  decomposition by excessive radiation).

Selective extraction of  $^{249}\text{Bk}$  using a dual column of MP-1/LN resins in a common mobile effluent of 8 M  $\text{HNO}_3$ –0.5 M  $\text{NaBrO}_3$  is a successful example of making one of the stacked columns behave as a “cherry picker” to obtain the goal actinide. Not every dual-column design must achieve such a success, but the design should at least improve the goal actinide separation by media change or acidity change and should avoid time-consuming operations such as drying downs for feed preparations. The next section describes the  $^{230}\text{U}$  separation from Th, Pa, and FP demonstrating broad applicability.

## $^{230}\text{U}$

### Demand and Production of $^{230}\text{U}$ (20.8 d)

The use of  $\alpha$ -emitting radionuclides for treatment of human diseases is referred to as targeted alpha therapy (TAT). Because  $^{223}\text{RaCl}_2$  has proven to be effective in clinical studies for treatment of hormone-refractory prostate cancer metastasized to bone [8, 9], other  $\alpha$ -emitting radionuclides with similar half-lives, including  $^{212}\text{Bi}$  (60.55 min),  $^{213}\text{Bi}$  (45.61 min, the granddaughter of  $^{225}\text{Ac}$ ) and  $^{226}\text{Th}$  (30.57 min, daughter of  $^{230}\text{U}$ ), are under intensive study. Among them,  $^{226}\text{Th}$  has been selected in a collaborative project by University of Washington, ORNL, and Los Alamos National Laboratory (LANL) for the following reasons:

1. Same as other  $\alpha$ -emitter candidates,  $^{226}\text{Th}$  possesses high linear energy transfer (LET), which results in cell killing that is not dependent on dose rate, oxygen tension, or radiosensitivity of the targeted cancer cells [10].
2. Among the two generator pairs ( $^{225}\text{Ac}/^{213}\text{Bi}$  and  $^{230}\text{U}/^{226}\text{Th}$ ),  $^{230}\text{U}$  (20.8 d), the mother nuclide of  $^{226}\text{Th}$ , has a relatively longer half-life than  $^{225}\text{Ac}$  (10.0 d), the grandmother of

$^{213}\text{Bi}$ , is suitable for building  $^{230}\text{U}/^{226}\text{Th}$  generators, making the therapeutic radiopharmaceutical consistently available in a clinical setting.

3.  $^{226}\text{Th}$  decay promptly releases four alpha particles before reaching  $^{210}\text{Pb}$  (22.20 y), while decaying  $^{213}\text{Bi}$  releases only one alpha before transitioning to stable  $^{209}\text{Bi}$ . The  $^{230}\text{U}/^{226}\text{Th}$  generator is expected to play an important role in combined immunotherapy and alpha radiation therapy.

$^{230}\text{U}$  is indirectly produced at the University of Washington by relatively low-energy proton irradiation of  $^{232}\text{Th}$  metal foil target via the reaction of  $^{232}\text{Th} (p, 3n)^{230}\text{Pa} \xrightarrow{\beta^-} {}^{230}\text{U}$ , where  $^{230}\text{U}$  is the decay daughter of  $^{230}\text{Pa}$  (17.4 d), as shown in **Fig. 10**.

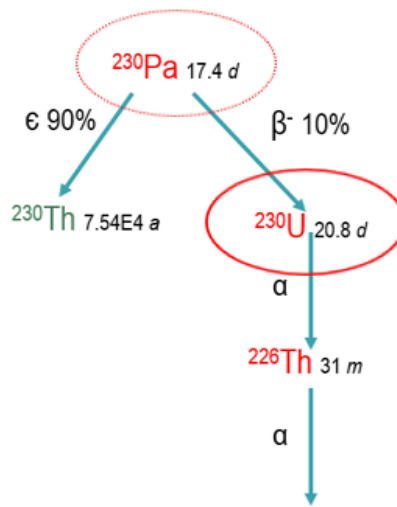


**Fig. 10.** Decay chain of the direct irradiation product of  $^{230}\text{Pa}$ .

University of Washington and LANL colleagues collaborate on the selection of target and bombardment energy. Since 2020, five  $^{232}\text{Th}$  metal targets have been irradiated by proton beam of 1, 3, 5 10 and 22  $\mu\text{A} \cdot \text{hr}$ . ORNL's task has been to design a fast separation route to recover  $^{230}\text{U}$  and  $^{230}\text{Pa}$  and then ship the purified  $^{230}\text{U}$  back to the university for further studies of  $^{230}\text{U}/^{226}\text{Th}$  generator and  $^{226}\text{Th}$  chelating.

### Separation of Chemical Elements from Irradiated Th Matrices

$^{230}\text{U}$  is the number-one goal actinide to be separated from  $^{232}\text{Th}$ ,  $^{230}\text{Pa}$ , and numerous FP impurities in this separation scheme design. Nuclear chemists have had a general impression that uranium separation is a mature topic in nuclear chemistry because the PUREX process was created 60 years ago and many new resins (e.g., U-TEVA) have been manufactured in recent years. The case of  $^{230}\text{U}$  separation has a few exceptional requirements that must be considered:

1.  $^{230}\text{U}$  has short half-life than most other cases of uranium separations.
2. The target of Th metal requires a dissolution in high HCl spiked with hydrofluoric acid (HF), not the common  $\text{HNO}_3$  media. One may argue for changing the HCl media to

$\text{HNO}_3$  and then performing U separation, but solution media change is commonly the most time-consuming step in chemical processing and should be avoided, especially with short-half-life isotope products.

3. In this processing scheme,  $^{230}\text{Pa}$  is the secondary isotope product to be separated. The recovered  $^{230}\text{Pa}$  is indeed the source for harvesting the ingrowth  $^{230}\text{U}$ .
4. The designed separation scheme should also achieve separation of 190 FP impurities (per ORIGEN calculation). In the case of treatment of five targets, only  $\sim 20$  radioactive impurities were detected in sample analyses (e.g.,  $^{95}\text{Nb}$ ,  $^{95}\text{Zr}$ ,  $^{103}\text{Ru}$ ,  $^{140}\text{La}$ ,  $^{155}\text{Eu}$ ). The high chemical purity of the  $^{230}\text{U}$  product (free of  $^{232}\text{Th}$  and other impurity metal ions) is the guarantee for follow up  $^{226}\text{Th}$  chelation study.

In previous work [11–16], five different resins were examined for their performance in uranium extraction or separations from other isotopes, especially in HCl media (Table 4).

**Table 4.** Literature  $K_d$  values of isotopes of interest with resins in HCl or  $\text{HNO}_3$  media [11–16].

$K_d$ (media)	10 M HCl (feed)	6 M HCl	4 M HCl	$\leq 1$ M HCl	$\leq 1$ M $\text{HNO}_3$
$\text{Pa}^{\text{V}}$ on TEVA	$10^5$	<u>90, 500</u>	<u>8, 10<sup>2</sup></u>	<u>8, 80</u>	<u>2, 80</u>
$\text{U}^{\text{VI}}$ on TEVA	$10^3$	$10^3$	$8 \times 10^2$	$< 10$	2
$\text{Th}^{\text{IV}}$ on TEVA	$< 1$	$< 1$	$< 1$	$< 1$	70
$\text{Pa}^{\text{V}}$ on TRU	$10^4$	$2 \times 10^4$	$10^3$	$10, 10^2$	$3 \times 10^2$
$\text{U}^{\text{VI}}$ on TRU	$10^3$	$3 \times 10^3$	$3 \times 10^3$	$10^2, ?$	$10^3$
$\text{Th}^{\text{IV}}$ on TRU	$10^4$	$2 \times 10^4$	$10^3$	$1, ?$	$10^4$
$\text{Pa}^{\text{V}}$ on UTEVA	$10^4$	20	4	$< 2$	10
$\text{U}^{\text{VI}}$ on UTEVA	80	$2 \times 10^2$	60	1	70
$\text{Th}^{\text{IV}}$ on UTEVA	$10^2$	1	0.2	$< 0.1$	20
$\text{Pa}^{\text{V}}$ on AX	$10^5, 10^3$	$10^3, 10$	$10^2, 5$	$6-20, ?$	$10, 2$
$\text{U}^{\text{VI}}$ on AX	$10^3$	800	180	2	$< 2$
$\text{Th}^{\text{IV}}$ on AX	$< 1$	$< 1$	$< 1$	$< 1$	$< 1$
$\text{Pa}^{\text{V}}$ on TK400	$90, \geq 10^3$	$2.2, 300$	$< 1, 200$	$1.3, 10^2$	$?, 90$
$\text{U}^{\text{VI}}$ on TK400	4.2	1.5	1.5	1.5	?
$\text{Th}^{\text{IV}}$ on TK400	$< 1$	1.2	1.6	2.4	?

In the solution of dissolved  $^{232}\text{Th}$  target, Th is in the largest mass amount (0.9 g) vs. produced actinides and impurities, so as to be removed first. Among the resin candidates in Table 3, TEVA and AX resins may retain both U and Pa (in high HCl) while allowing Th to go through the resin column. Comparing the two, AX resin is considered more radiation resistant in the context of dealing with dissolved irradiated target of high dose. Therefore, AX resin (MP-1 resin in this work) was chosen to build the primary column for separating Th from U and Pa.

Prior to receiving irradiated  $^{232}\text{Th}$  targets, tracer tests with available  $^{234}\text{U}$  and  $^{233}\text{Pa}$  were performed to confirm their retention on MP-1 column and to select the proper conditions for the

follow-up separation of U and Pa. The concentration of HCl ([HCl]) varied from 9 to 10 M, while the concentration of hydrofluoric acid ([HF]) of the feed and effluent varied within 0.266 M. The final selected feed and mobile effluent conditions are 10 M HCl–0.00266 M HF. Because dissolution of 0.9 g of Th metal foil requires more HF addition, the dissolved solution needs to be dried down and then brought up with 10 M HCl–0.0026 M HF for the column run. The selection of 10 M HCl–0.0026 M HF ensured not only that Pa and U were retained on the MP-1 resin column while removing 0.9 g Th off the column, but also nearly 100% of  $^{95}\text{Zr}$ ,  $^{137}\text{Cs}$ ,  $^{141,144}\text{Ce}$ ,  $^{140}\text{Ba}$ , and  $^{140}\text{La}$  and partial amounts of  $^{95}\text{Nb}$ ,  $^{103,106}\text{Ru}$ , and  $^{155}\text{Eu}$  were removed during the elution with 10 M HCl–0.0026 M HF.

The steps of the  $^{232}\text{Th}$  target processing include:

**(Fig. 11)**

1. Dissolve the irradiated  $^{232}\text{Th}$  metal foil by concentrated HCl spiked with a sufficient amount of HF.
2. Dry down the dissolved solution and bring up with 10 M HCl–0.0026 M HF.

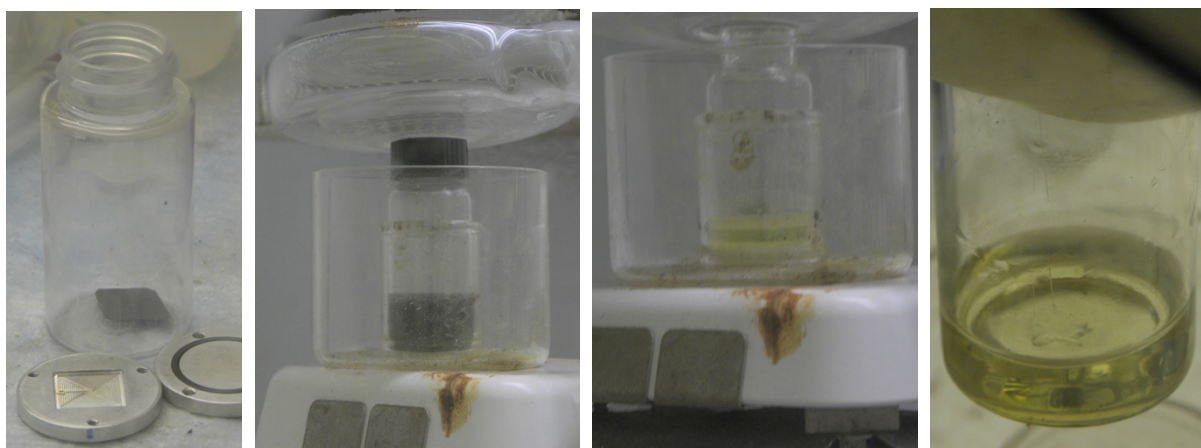


**Fig. 11.** Dissolution of irradiated Th target, drying down, and redissolution in 10 M HCl–0.00266 M HF.

**(Fig. 12)**

3. Load the feed onto the preconditioned MP-1 column and follow by elution with 10 M HCl–0.0026 M HF effluent (i.e., single-column run for Th and removal of most impurities with a loss of tiny amounts of  $^{230}\text{U}$  and  $^{230}\text{Pa}$ ), collected in the bottle marked “FLR.”
4. Add 10 M HCl–1.4125 M HF effluent onto the MP-1 column to selectively elute Pa off the MP-1 column (with partial  $^{95}\text{Nb}$ ,  $^{103,106}\text{Ru}$ , and a majority of  $^{243}\text{Am}$  off) into the bottle marked “Pa.”

The remaining species on MP-1 includes almost all the  $^{230}\text{U}$  and >50% of original  $^{95}\text{Nb}$  and a small portion of  $^{103}\text{Ru}$  and  $^{155}\text{Eu}$ . Up to this point, a single MP-1 column completed the separation of actinides Th, Pa, and U, although other impurities were distributed among the three

actinides. The dual-column technique improves the purity of the  $^{230}\text{U}$  product, changes its media from HCl to  $\text{HNO}_3$ , and then lowers its acidity for easier drying-down.

5. Attach a pre-conditioned DGA column to the top MP-1 column that contains  $^{230}\text{U}$ . Elute the stacked columns of MP-1/DGA with 10 M  $\text{HNO}_3$ , where  $^{230}\text{U}$  is eluted off the MP-1 column but then retained onto the DGA column in 10 M  $\text{HNO}_3$ . During the 10 M  $\text{HNO}_3$  elution, majority of the remaining  $^{95}\text{Nb}$ ,  $^{103}\text{Ru}$  and  $^{155}\text{Eu}$  are washed away from the  $^{230}\text{U}$  on the DGA column. The 10 M  $\text{HNO}_3$  wash is collected into the bottle marked “Pre-U”.
6. Detach the DGA column which contains the purified  $^{230}\text{U}$  and strip  $^{230}\text{U}$  off with 0.5 M  $\text{HNO}_3$ , collected into the bottle marked “U-230”.
7. Slowly dry down the  $^{230}\text{U}$  solution of low  $\text{HNO}_3$  after transfer into a V-vial. Only the dry U nitrate salt is qualified for shipping.

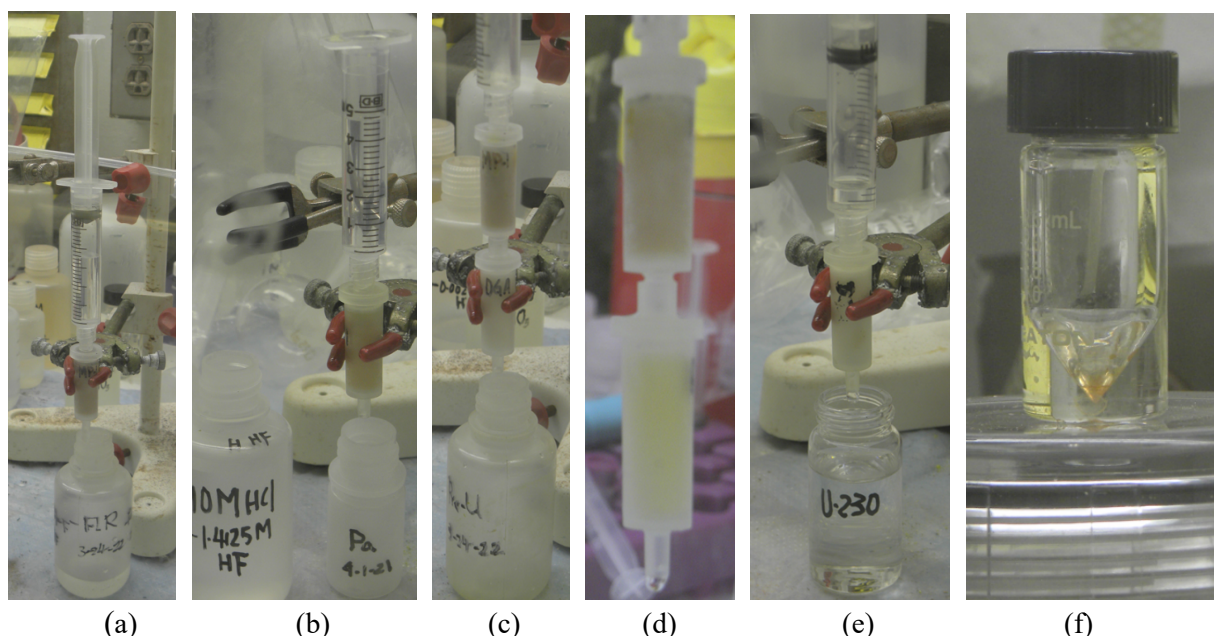


**Fig. 12.** Column-run process. (a) Th removal, (b) elute Pa, (c) transfer U to DGA, (d) yellow U color on DGA column, (e) strip  $^{230}\text{U}$  off DGA, (f) dried  $^{230}\text{U}$  nitrate salt for shipping.

It is noted that in the case of  $^{230}\text{U}$  separation from Pa and Th, the primary separation of the three actinides is achieved by using MP-1 column, while the follow-up dual-column further purifies the  $^{230}\text{U}$  product by removing residual impurities and modifies the media to desired composition.

As with  $^{249}\text{Bk}$ , only one feed preparation is required for the entire process, which made it a rapid separation process. The above column run takes only 2 h, while the drying down of dissolved target solution takes 6 h. The most time-consuming step in this process,  $\sim 24$  h, is the dissolution of the irradiated Th metal foil.

A schematic diagram for the entire process is shown in **Fig. 13**.

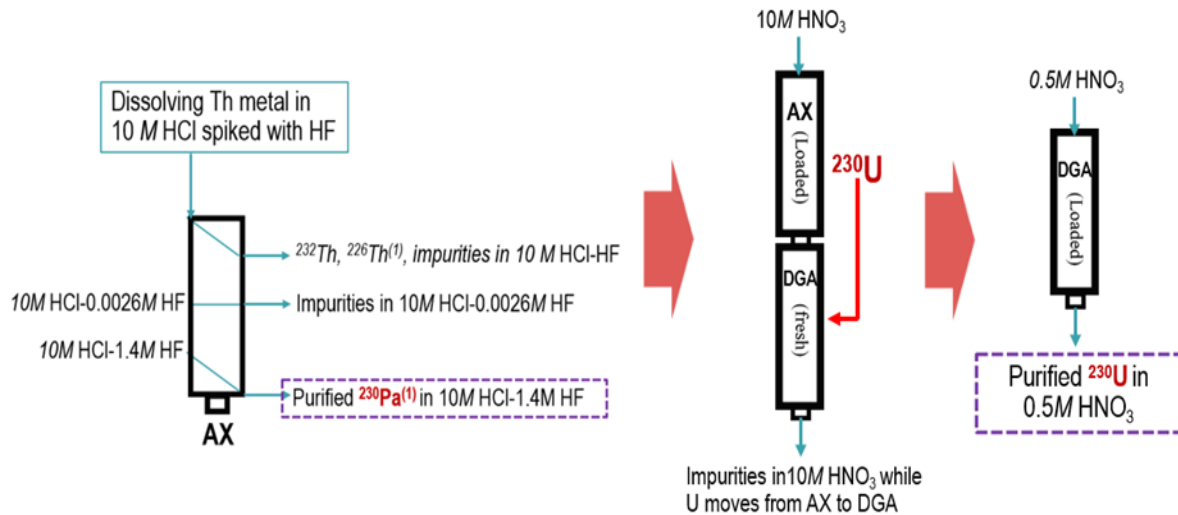


**Fig. 13.** Schematic diagram for rapid separation of  $^{230}\text{U}$  from  $^{230}\text{Pa}$ ,  $^{232}\text{Th}$ , and FP impurities.

The  $^{230}\text{Pa}$  and some impurities in the bottle marked “Pa” will be processed after a period for  $^{230}\text{U}$  ingrowth by drying down the solution of 10 M HCl–1.4125 M HF and bringing back with 10 M HCl–0.00266 M HF solution to repeat the process shown in Fig. 13 for ingrowth  $^{230}\text{U}$  recovery.

So far, five irradiated  $^{232}\text{Th}$  targets have been treated at ORNL(Table 5), and three more will be irradiated at much higher  $\mu\text{A}.\text{hr}$  with a higher content of FP impurities.

**Table 5.**  $^{230}\text{U}$  product purified/recovered from irradiated  $^{232}\text{Th}$  target at ORNL since 2020.

Irradiation of Th232 Target		Recovered U230 from the feed			Note
	$p$ Beam	Bq	uCi	% of total	
<b>1<sup>st</sup> Th232</b>	1 $\mu\text{A}.\text{hr}$	3.24E4	<b>0.88</b>	31%	Method Optimization
<b>2<sup>nd</sup> Th232</b>	3 $\mu\text{A}.\text{hr}$	2.02E5	<b>5.45</b>	99.4%	
<b>3<sup>rd</sup> Th232</b>	5 $\mu\text{A}.\text{hr}$	1.87E5	<b>5.06</b>	91%	
<b>4<sup>th</sup> Th232</b>	15 $\mu\text{A}.\text{hr}$	6.10E5	<b>16.49</b>	93.3%	Shipped to UW
<b>5<sup>th</sup> Th232</b>	22 $\mu\text{A}.\text{hr}$	1.17E6	<b>31.68</b>	99.3%	Shipped to UW

UW = University of Washington

In our experience, this quick separation scheme by mixed single- and dual-column method worked well. With higher irradiation intensity (up to 80  $\mu\text{A}.\text{hr}$ ), the workload for separating more FP impurities will increase. The current procedure is qualified to separate the three actinides as needed, but small traces of FP impurities still contaminate the  $^{230}\text{U}$  product (see **Fig. 14** and **Table 6**).

Fig. 14 displays the separation profile of  $^{230}\text{U}$ ,  $^{230}\text{Pa}$  and radioactive impurities in the combined column runs (single MP-1, dual MP-1/DGA, and single DGA) for fifth  $^{232}\text{Th}$  target treatment, while in **Table 6**, the percentage of each isotope distribution among the fractions is based on the sum of each isotope amount from all column-run fractions, not on the data for the dissolved target solution. Indeed, a larger error would be introduced otherwise due to the volume of the 0.9

g of solid in only 3 mL of solution. Some undissolved white foam floating in the 3 mL solution added more uncertainty to the analytical data of this solution.

#### Column Runs of U/Pa/Nb/Ru/etc (Normalized to 1)

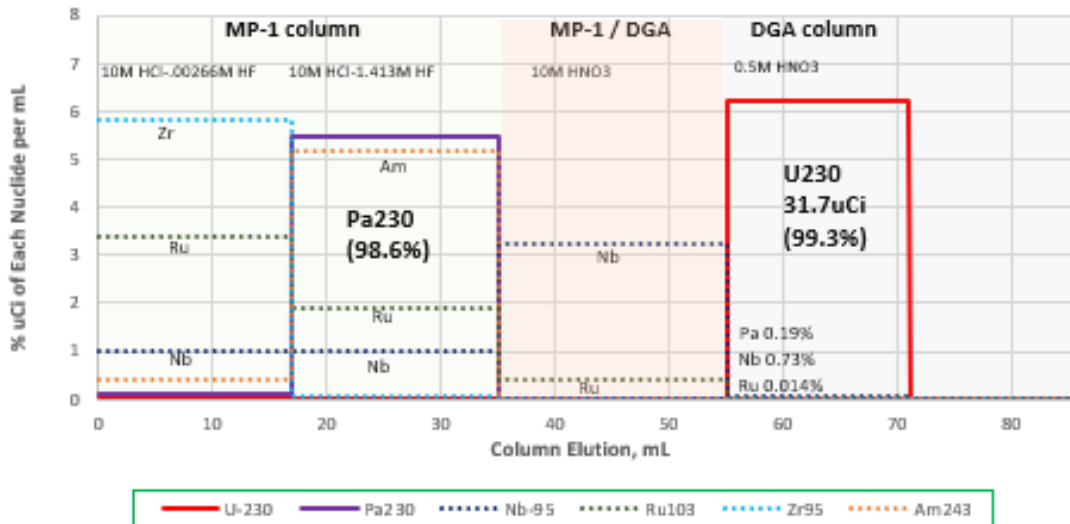


**Fig. 14** Separation profile of  $^{230}\text{U}$ ,  $^{230}\text{Pa}$  and impurities from fifth target by column runs. (Note: the non-rad  $^{232}\text{Th}$  and those being completely removed by 10 M HCl-0.00266 M HF are not plotted in Fig. 14.)

**Table 6.** Isotope distribution among the column-run fractions in fifth Th target treatment.

	10 M HCl- 0.00266 M HF	10 M HCl- 1.4125 M HF	10 M HNO <sub>3</sub>	0.5 M HNO <sub>3</sub>	Sum of fractions
<b>Vol. (mL)</b>	16.98	18.0	20.0	16.0	
$^{230}\text{U}$ (Bq)	8609	0	0	1.172E6	31.68 $\mu\text{Ci}$
% Total	0.729	0	0	99.271	100
$^{230}\text{Pa}$ (Bq)	407520	2.88E7	0	7040	242 $\mu\text{Ci}$
% Total	1.395	98.581	0	0.024	100
$^{95}\text{Nb}$ (Bq)	1.56E5	1.60E5	5.80E5	6560	6.21 $\mu\text{Ci}$
% Total	17.299	17.747	64.228	0.726	100
$^{103}\text{Ru}$ (Bq)	1.02E6	6.12E5	1.38E5	3840	14.81 $\mu\text{Ci}$
% Total	57.474	34.525	7.785	0.217	100
$^{95}\text{Zr}$ (Bq)	2.04E6	2.34E4	0	0	25.93 $\mu\text{Ci}$
% Total	98.865	1.135	0	0	100
$^{140}\text{Ba}$ (Bq)	3.23E6	9.72E4	0	0	12.26 $\mu\text{Ci}$
% Total	97.075	2.925	0	0	100
$^{243}\text{Am}$ (Bq)	1.27E4	1.80E5	0	0	26.17 $\mu\text{Ci}$
% Total	6.571	93.429	0	0	100
<b>100% removed by 10 M HCl-0.00266 M HF includes <math>^{141,144}\text{Ce}</math>, <math>^{140}\text{La}</math>, and <math>^{137}\text{Cs}</math>.</b>					

The  $^{230}\text{U}$  product, obtained from fifth  $^{232}\text{Th}$  target, contains 99.3% of  $^{230}\text{U}$  from all fractions, but also contains minor amounts of  $^{230}\text{Pa}$  (0.024%),  $^{95}\text{Nb}$  (0.726%), and  $^{103}\text{Ru}$  (0.217%), which indicates opportunities for future improvement; for example, the detached LN column could be

eluted with more 10 M HNO<sub>3</sub> to remove the residual <sup>95</sup>Nb and <sup>103</sup>Ru, or the dual column could be eluted with more 10 M HCl–1.4125 M HF to remove the residual <sup>230</sup>Pa from the <sup>230</sup>U on column.

## Conclusion

When more than three actinides of interest must be separated via a single process, the CX-AHIB method is invaluable. However, when fewer than three are involved, other separation methods are preferred due to the tedious steps and strict requirements on process controls associated with CX-AHIB.

Our research demonstrated the feasibility of a rapid and more efficient dual-column method for separating a actinide of interest from others. Examples of <sup>249</sup>Bk and <sup>230</sup>U show that a good dual-column design will help achieve rapid separation of an actinide of interest from other actinides and impurities once the following required conditions are met:

1. Two right resins are selected.
2. A proper common mobile effluent is identified.
3. Attachable columns can be fabricated with features for dimension (volume and length/diameter) and temperature requirements.
4. A proper way to drive the mobile effluent using a syringe, Ar over pressure, or other methods.

The success of a dual column design can be judged to different levels. The top level would be making one of the stacked columns a “cherry picker” for the actinide of interest, away from other f-elements and impurities. Secondary success of the design would be helpful in further purification of the actinide of interest from others. At the very least, the dual-column design should help in desired media or acidity changes with no need to dry down the solution.

Use of a good design of dual column speeds up separation of the actinide of interest from other actinides and impurities or shortens the processing steps via reduced numbers of feed preparation and media changes.

## Acknowledgments

This research is supported by the US Department of Energy Isotope Program, which is managed by the Office of Science for Isotope R&D and Production.

We acknowledge Los Alamos National Laboratory and the University of Washington for the <sup>232</sup>Th foil preparation and the proton irradiation of the target for production of <sup>230</sup>Pa and <sup>230</sup>U. Also, we acknowledge ORNL HFIR for their continued support to Cf-252 program.

## References

1. Choppin GR and Silva RJ; *Separation of the Lanthanides by Ion Exchange with Alpha-hydroxy Isobutyric Acid*, University of California–Berkeley report no. UCRL-3265, January 1956.
2. Robinson SM, Benker DE, Collins ED, Ezold JG, Garrison JR and Hogle SL, “Production of Cf-252 and Other Transplutonium Isotopes at Oak Ridge National Laboratory,” *Radiochim Acta* 108(9) (2020): 737–746.
3. Baybarz RD, Knauer JB, Orr PB, “Final Isolation and Purification of the Transplutonium Elements from the Twelve Campaigns Conducted at TRU during the Period August 1967 – December 1971”, ORNL Report 4672 UC-4, April 1973
4. Peppard DF, Moline SW and Mason GW (1957), “Isolation of Berkelium by Solvent Extraction of the Tetravalent Species,” *J Inorg Nucl Chem* 4 (1957): 344–348.
5. Du M, Tan R, Boll R, *Application of a Dual Column Method to Selectively Extract and Purify Bk-249 from Other Actinides and Impurities*, ORNL report no. ORNL/TM-2019/1138, September 2019.
6. Moore FL, “New Method for Rapid Separation of Bk (IV) from Ce (IV) by Anion Exchange,” *Anal Chem* 39 (1967): 1874–1876.
7. Makarova TP, Fridkin AM, et al. “Electromigration of Bk (IV) and Some Other Tetravalent Cations in Nitric Acid Solutions,” *J. Radioanal Chem* 53 (1–2) (1979): 17–24.
8. Nilsson S, Strang P, Aksnes AK, Franzen L, Olivier P, et al. “A Randomized, Dose-Response, Multicenter Phase II Study of Radium-223 Chloride for the Palliation of Painful Bone Metastases in Patients with Castration-Resistant Prostate Cancer,” *Eur J Cancer* 48 (2012): 678–686.
9. Parker C, Heinrich D, O’Sullivan JM, Fossa S, Chodacki A, et al., “Overall Survival Benefit of Radium-223 Chloride (Alpharadin) in the Treatment of Patients with Symptomatic Bone Metastases in Castration-Resistant Prostate Cancer (CRPC): A Phase III Randomized Trial (ALSYMPCA),” *Eur J Cancer* 47 (Suppl2), 3 (abstract), 2012.
10. Hall, EJ and Giaccia AJ, *Radiobiology for the Radiologist*, 6th ed., Lippincott Wilkins & Williams, Philadelphia, USA, 2006, ISBN: 0-7817-4151-3
11. Mendes M, Aupiais J, Jutier C, and Pointurier F, “Determination of Weight Distribution Ratios of Pa(V) and Np(V) with Some Extraction Chromatography Resins and the AG1-X8 Resin,” *Anal Chim Acta* 780 (2013): 110–116.
12. Skinner M and Knight D, “The Behavior of Selected Fission Products and Actinides on UTEVA Resin,” *J Radioanal Nucl Chem* 307 (2016): 2549–2555.

13. Ostapenko V, Sinenko I, Arefyeva E, Lapshina E, and Ermolaev S, “Sorption of Protactinium (V) on Extraction Chromatographic Resins from Nitric and Hydrochloric Solutions,” *J Radioanal Nucl Chem* 311(2), (2017): 1545–1550
14. Vajda N, Molnar Z, and Osvath S, “Use of UTEVA for the Separation of Th, U, Np and Pu,” Presentation at Eichrom European Users’ Meeting, Vienna, Austria, June 7, 2002.
15. Pourmand A and Dauphas N, “Distribution Coefficients of 60 Elements on TODGA Resin: Application to Ca, Lu, Hf, U and Th Isotope Geochemistry,” *Talanta* 81 (2010): 741–753.
16. Knight AW, Eitrheim ES, Nelson AW, Nelson S and Schultz MK, “A Simple-Rapid Method to Separate Uranium, Thorium, and Protactinium for U-Series Age-Dating of Materials,” *J Environ Radioactiv* 134 (2014): 66–74.